THE ARCHIVE OF MECHANICAL ENGINEERING

VOL. LVIII 2011 Number 2

10.2478/v10180-011-0017-3

Key words: glider, crash tests, structure's damage, numerical model

LUKASZ LINDSTEDT *

NUMERICAL SIMULATION OF GLIDER CRASH AGAINST A NON-DEFORMABLE BARRIER

This study, describing computer simulation of a glider crash against a non-deformable ground barrier, is a part of a larger glider crash modeling project. The studies were intended to develop a numerical model of the pilot – glider – environment system, whereby the dynamics of the human body and the composite cockpit structure during a crash would make it possible to analyze flight accidents with focus on the pilot's safety. Notwithstanding that accidents involving glider crash against a rigid barrier (a wall, for example) are not common, establishing a simulation model for such event may prove quite useful considering subsequent research projects. First, it is much easier to observe the process of composite cockpit structure destruction if the crash is against a rigid barrier. Furthermore, the use of a non-deformable barrier allows one to avoid the errors that are associated with the modeling of a deformable substrate, which in most cases in quite problematic. Crash test simulation, carried out using a MAYMO package, involved a glider crash against a wall positioned perpendicularly to the object moving at a speed of 77 km/h. Computations allowed for determination of time intervals of the signals that are required to assess the behavior of the cockpit and pilot's body – accelerations and displacements in selected points of the glider's structure and loads applied to the pilot's body: head and chest accelerations, forces at femur, lumbar spine and safety belts. Computational results were compared with the results of a previous experimental test that had been designed to verify the numerical model. The glider's cockpit was completely destroyed in the crash and the loads transferred to the pilot's body were very substantial – way over the permitted levels. Since modeling results are fairly consistent with the experimental test, the numerical model can be used for simulation of plane crashes in the future.

1. Introduction

The past two decades saw a substantial increase of interest in glider flight safety issues, with focus not only on performance but also on regulations

* *Institute of Aeronautics and Applied Mechanics, Warsaw University of Technology, ul. Nowowiejska 24, 00-665 Warsaw, Poland; e-mail: luclin@meil.pw.edu.pl*

specifying pilot's safety requirements to be met by the structure of the glider. These regulations, as contained in the standard CS-22 (JAR-22) [1], describe safety requirements that should be satisfied by a glider during normal and the so-called „hard" landing. Nevertheless, the requirements and procedures for pilot safety testing at crash landing are still to be developed.

Several factors have contributed to this situation, including a relatively limited number of glider users and high costs of crash tests, which are prohibitive to glider manufacturers. Moreover, due to a relatively few fatal accidents [2-6] the issue is not considered as a serious public problem.

A rapid development of IT technology over the past years made it possible to investigate flight crashes using numerical testing methods. Sophisticated computational packages, such as MADYMO, provided advanced tools for delivery of dynamic studies.

Nevertheless, considering the complexity of aeronautic structures and a highly complicated behavior of composites, especially under fast changing loads of a very high amplitude, several model simplification assumptions are required, in particular if the tested composite structures are subjected to destructive loads. For samples with relatively simple shapes and loads applied in a typical way, modeling yields quite reliable results (in comparison with experimental tests) [7-12], but adequate modeling of a large and complex structure, such as a glider, is still a huge challenge. The application of excessively complex material models combined with numerical limitations often leads to instability of simulation, while oversimplification causes non-physical behavior of the model under investigation [13].

The investigations presented in this study on the simulation of glider crash against a rigid barrier were intended to develop a model that would allow for the development of a relatively reliable crash model, while keeping it as simple as possible to facilitate its efficient use. In spite of all benefits associated with the application of numerical methods, it is obvious that simulation tests are not expected to replace experimental tests as a reference for the verification of numerical models. Therefore, computer simulation described herein was preceded by an experimental crash test [17]. The results of that test were subsequently used for an quality assessment of the model.

2. Methods

2.1. Glider's model

The numerical model of the glider is based on the mock-up model of the PW-5 glider.

Glider cockpit, a limited space restricting pilot's movements and maneuvers, but protecting him against the elements, is the decisive component of glider's structure in terms of pilot's safety. Therefore, the pilot cockpit was reproduced strictly according to the technical documentation as the most important component of the numerical model. Only the gauges and the radio were omitted, leaving just bare external shell of the control panel, which the pilot may potentially hit.

The tail section of the glider was omitted and replaced by a carriage of a mass similar to that of the tail section. The carriage was moving the cabin during the experimental test. The wings were modeled using a steel wing spar with weights suspended thereto to simulate the weight of the wings. The mass of the model differed from that of the mock-up model by roughly 5%. The model of the glider's front section is shown with a dummy pilot in Figure 1.

Fig. 1. Glider's model

Glider cockpit model is composed of a total of 85785 nodes that form 87545 four-node shell elements. In addition, the control panel was modeled using the so-called "facet-surface"* and defining 1926 nodes and 1834 elements. Two elements of the structure were excluded from the 'global' MES model, due to a negligible risk of destruction (according to experimental tests), and modeled on a facet basis to reduce computation time without any adverse effect on contact properties. The elements in question are: seat

* The method consists in defining surface area of the modeled segment using a grid of elements, like in the case of finite element method. The key difference is that these elements are used solely for contact analysis that allows for correct definition of force interactions with adjacent elements; a segment is treated as a single rigid body in equations describing motion of the entire system.

bucket – 9305 nodes and 8998 elements and the backrest – 4782 nodes and 4850 elements. The entire set was divided into 46 'components', mainly for functional reasons, such as interconnections between larger components of the structure, contact interactions and variable properties of the elements, etc..

Cockpit shield, which is of significance during a crash (as it stiffens the structure to some degree), was another MES-modeled element of the cockpit. The cockpit shield model was composed of a total of 16455 nodes that form 16774 four-node shell elements. It was sub-divided for functional reasons into three components. In addition, the mechanism attaching the cockpit to the body was rendered, in a simplified way, using the method of multi-component systems.

The method of multi-component systems was also used to model the glider's carriage, including wheels, front undercarriage wheel, control stick, wing spar with weights and fastening bolts, as well as with safety belt fastener anchoring points. The application of the multi-component simulation method was in that case reasonable, since the aforementioned structures were poorly susceptible comparing to other elements of the structure (the carriage, wing spar, metal boxes with weights and belt fasteners) or their precise rendering was not required for good performance of the entire model. A gain in computation time was a substantial and measurable benefit from that approach.

The PW-5 glider mock-up, as described above, allowed for precise reconfiguration of the pilot's immediate environment (the cockpit) and good rendering of the total glider's weight, which depending on actual equipment amounted to approx. 185 kg. Nevertheless, the mock-up presented several limitations.

The replacement of the rear body section (tail spar with tail fin) with a carriage and substitution of wings for a spar with weights attached thereto did not affect the glider's center of gravity but resulted in a significant change in mass layout and geometry, which considerably affected the moment of inertia. As a consequence, the model was suitable for frontal and 'symmetric' crash tests only (with movement along the body's plane of symmetry), wherein any lateral rotation was absent. Wing representation as a rigid spar with weights, which prevented an insight into the impact of wing vibrations on the structure's dynamics (quite substantial, according to available evidence) was another weakness of the model. Moreover, this approach to the wing structure rendering did not allow for investigation into pilot's threat from wings and their fastening during a crash (as reported from actual events). Another limitation arising from model assumption was the omission of research into aerodynamic impacts. It was assumed that the impact of aerodynamic forces on glider's behavior was relatively small upon landing,

but before the crash occurrence. This simplifying assumption might seem understandable if we consider that the experimental tests, as required for the verification of theoretical studies, were conducted in laboratory conditions, wherein the influence of atmospheric conditions (such as for example a wind burst) has been eliminated and glider's structure elements that were decisive in its aerodynamics (wings and tail) were significantly simplified.

A model of isotropic material with a module describing destruction by brittle cracking was used for the modeling of material properties of the glider's shell and cockpit.

In the case of cockpit made of plexiglass (polymethyl methacrylate – PMMA), the assumption of isotropy seems reasonable[**], but for a composite material this is a very serious simplification. The justification behind this approach is that the model itself is a large and very complex composite structure, which requires time-consuming computations and very powerful computers. Another serious problems are associated with an in-depth investigation of non-isotropic properties of composite materials and their modeling, as well as with achieving stability in the case of more complex material models [13]. Material data presented in the Table 1 have been assumed in the simulation.

Table 1.

Assumed material constants

Constant	Glider shell	Cockpit shield
E	2.1E10 Pa	3.3E9 Pa
ν	0.3	0.37
ρ	1790 kg/m^3	1190 kg/m^3

In the light of aforementioned premises, numerical modeling of the structure based on isotropic material model can be considered as a justified approach. However, the omission of the destruction process description is intolerable, as this would lead to distorted and inconsistent with actual observations simulation results (e.g. extensive permanent deformations).

MADYMO allows us to introduce, for various types of material, a module describing material destruction that may occur under specified conditions [16]. The approach to the modeling of isotropic destruction occurring in a brittle material is described below.

The degree of destruction can be defined by the existing distribution and type of micro-defects. A local destruction can be determined by the

[**] The assumption of PMMA isotropy is derived directly from information provided by the manufacturers, which indicates a set of data for isotropic material including only two material constants.

proportion of the destructed to non-destructed area in the plane contained in a volume of the element. The ratio may range between 0 (no destruction) and 1 (total destruction). In the event of isotropic destruction, the degree of destruction can be expressed by the scalar value $D = D(x,t)$. The value is contingent on time $\boldsymbol{t}$ and energy status of the material $\boldsymbol{x}$. In the case of brittle fracturing, the propagation of destruction area is the only mechanism of energy dissipation. For isotropic destruction, the relationship between stresses and deformations is expressed as:

$$\underline{\sigma} = (1 - D)\,\underline{S}^0\underline{\varepsilon} \tag{1}$$

where: $\underline{S}^0$ – denotes the initial rigidity matrix

It is assumed that fracturing begins in a material on exceeding a critical thermodynamic value (energy density in a non-damage material), expressed by the following equation:

$$X = \frac{1}{2}\underline{\varepsilon}^T\underline{S}^0\underline{\varepsilon} \tag{2}$$

The rule of destruction zone propagation, as applied to the determination of structure degradation degree, is expressed as:

$$\dot{D} = \begin{cases} \dfrac{P_1 X^{P_2}}{(1-D)^{P_3}}\dot{X} & , X > \hat{X} \\ 0 & , \textit{otherwise} \end{cases} \tag{3}$$

where the current damage threshold is defined by the following equation:

$$\hat{X} = \max_{\tau \leqslant t} |X(\tau), X_0| \tag{4}$$

where X_0 denotes the boundary value of energy density in the non-damaged material that initiates the process of destruction, preceded by the occurrence of (user defined) critical deformation ε_0 that begins the process of destruction:

$$X_0 = \frac{1}{2}E(\varepsilon_0)^2 \tag{5}$$

In addition to the value of ε_0, the user must introduce to the fracturing model the parameters P_1, P_2 and P_3, which can be obtained from single-axis tests.

The difficulty lies in the fact that these parameters are not precisely interpreted in physical terms: they serve solely for model adjustment to the observed process of destruction. Obviously, the parameter P_1 must be higher than zero, since we assume that the process of destruction is irreversible. The

parameter P_2 is associated with the energy expended in fracture propagation, while P_3 is associated with the degree of damage at a particular moment.

Based on the results of a destructive test on a sample whose shape resembled that of glider's fore cone [17], as well as on the data concerning material properties of the composite and plexiglass, we adopted the values of damage process parameters shown in the Table 2.

Table 2.

Adopted model destruction parameters

Constant	Glider shell	Cockpit shield
ε_0	0.009	0.033
P_1	1.5E-7	1.5E-7
P_2	0	0
P_3	0	0

2.2. Dummy pilot

A numerical dummy model Hybrid II, used previously in experimental tests, was applied in modeling. In automotive industry, it was replaced by a new version Hybrid III, but Hybrid II is still being used for the purposes of aeronautical accident testing.

The dummy, which represents a 50-centile man, was experimentally verified for frontal loads (in automotive applications) and vertical loads (aeronautical applications) [14]. Dummy version of Hybrid II used in this study is a multibody model [15]. It is composed of more than 30 segments, of which external geometry (an important factor for proper modeling of contacts) is represented by over 50 (hyper)ellipsoids. Data on mass/inertia properties of the elements come from the tests and are described in the documentation. Data necessary for the determination of the ellipsoid's degree of exponent have been determined on the basis of technical drawings stored at the TNO research center.

An important advantage of the numerical dummy model is that the model is fitted with built-in sensors to record typical loads applied to the human body during the crash, and has pre-defined outputs of typical biomechanical risk measures, as used for evaluation of injury risk in crash biomechanics.

2.3. Non-deformable barrier model

A physical rigid barrier used in the experiment, which served as the basis for the numerical model, was in the form of a steel plate attached to a thick

concrete base. The barrier was fixed and – considering the glider structure's susceptibility – non-deformable.

Simplicity was the primary concern of the design of the non-deformable barrier model, while retaining certain features of the modeled barrier, especially those associated with its contact properties. These features were obtained by using the facet-surface technique.

The steel plate model composed of 1224 nodes forming 1151 elements was established from 1 cm thick shell elements affixed permanently in the inertial (absolute) system, in MADYMO called the Reference Space. Contact properties were simulated using a model of isotropic material with input values typical of steel elements: Young modulus – $E=2.1*10^{11}$ MPa, Poisson number – $\nu= 0.3$ and density – $\rho=7.85*10^3$ kg/m^3.

3. Results and discussion

3.1. Course of the test

As already mentioned above, computer simulation was intended to render a glider's crash against a non-deformable ground barrier at an initial velocity of 77 km/h.

Fig. 2. Selected frames from the experimental test video – $\Delta t=14$ ms

In order to substantiate the numerical model, animated simulation has been compared with the course of experimental test, as recorded using a high-speed camera. Crash simulation was limited to the first 70 milliseconds, after which the cockpit was completely demolished. After that time, any simulation would be purposeless from the viewpoint of model verification and for practical reasons (as the pilot would be crushed). Selected frames of the video (Fig. 2) and animation (Fig. 3) are presented below.

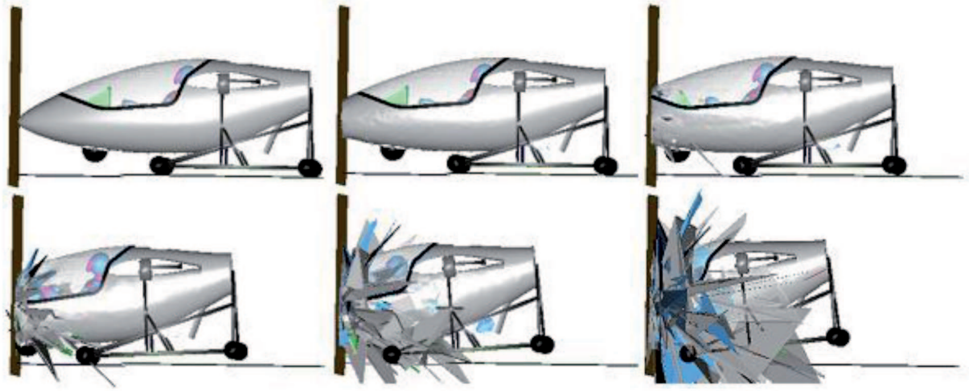

Fig. 3. Selected frames from computer simulation – Δt=14 ms

Considering that the risk of dummy destruction was high, a simplified dummy version representing only pilot's weight and size was used in the experimental test instead of normal, very expensive crash-test dummy. As a consequence, the signals directly related to the loads applied to the pilot's body were not measured during the test. Even in the absence of experimental verification, the results showing the loads transferred to the pilot's body provide valuable information on the total level of such loads and potential risks.

Crash pictures shown on Figures 2 and 3 clearly demonstrate that the glider hit the rigid barrier with extreme violence at 77 km/h. The entire process, significant from the viewpoint of the pilot's safety, lasted barely some 70 ms, or much less that in the case of a typical car crash. During that time the front section of the glider's composite cockpit has been almost completely destroyed up to the beginning of the seat bucket. Further on, a rotation of the entire structure can be seen, due to the layout of the crash test stand (this effect was rendered during the simulation). In the final phase it is clearly visible that, as a result of strong compression, the space required for pilot's survival was annihilated. This confirmed the concerns about the dummy (which in fact was destroyed during the experiment). A huge compression of the body can be seen at the simulation (Fig. 4).

Fig. 4. Strong compression of pilot's body during the crash against the wall (t=70 ms)

Although a "visual" comparisons of the behavior of the modeled structure during the experiment and simulation revealed strong similarities, we decided to compare the kinematics of the movements of selected points in the structure (video recording of displacements) with their respective nodes of the MES model (see Figure 5). Four characteristic points of the structure, easily identifiable on the basis of video records, were analyzed. Respective displacements of two best visible points that are relatively distant from each other were chosen for comparison: the so-called **markers** designated as M1 and M4.

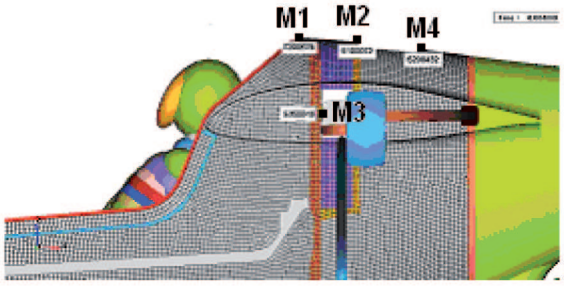

Fig. 5. Nodes selected for kinematics analysis

The displacements of the M1 marker are shown in Figures 6 and 7, while those of M4 marker are presented in Figures 8 and 9. In the case of displacements along the direction of movement, a great similarity between kinematics analysis and computer simulation of displacement curves was revealed for both markers.

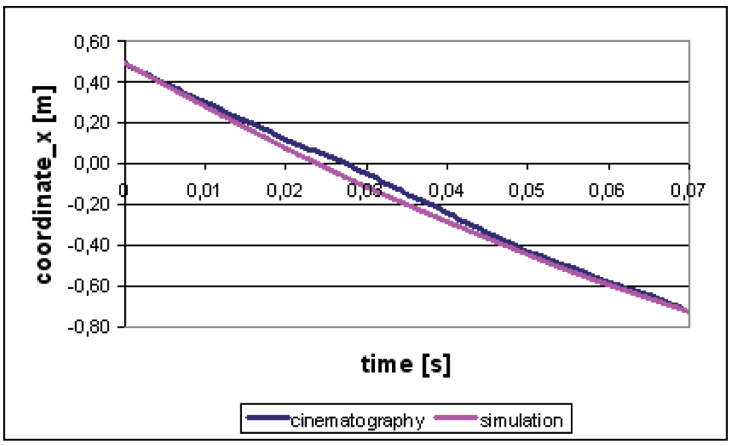

Fig. 6. Displacement of M1 marker along the direction of motion

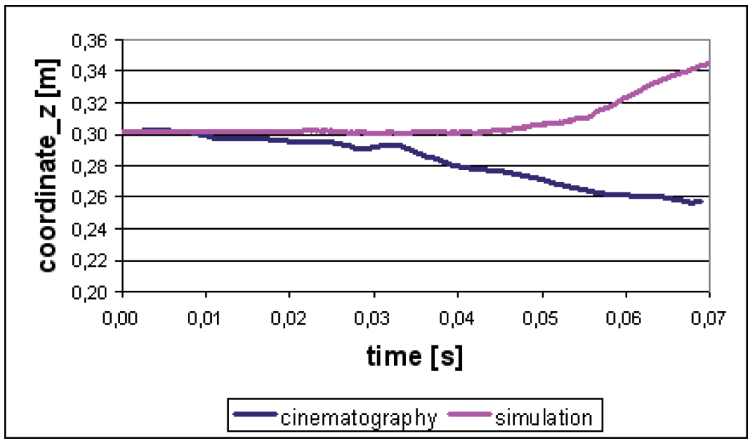

Fig. 7. Vertical displacement of M1 marker

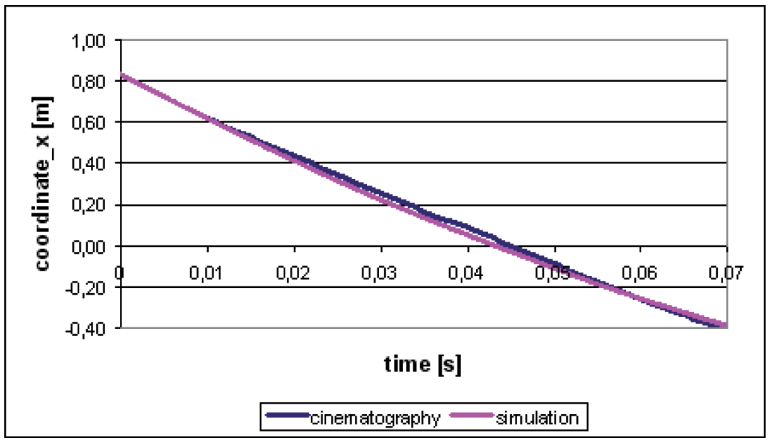

Fig. 8. Displacement of M4 marker along the direction of motion

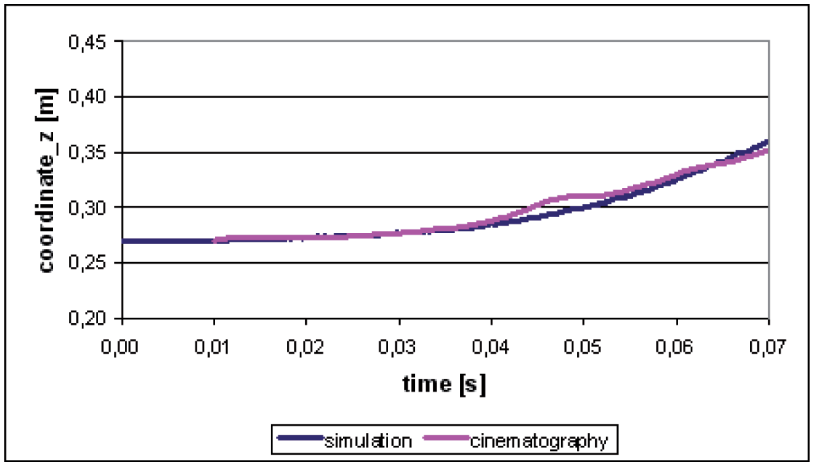

Fig. 9. Vertical displacement of M4 marker

A very interesting fact can be observed when analyzing the vertical displacement of the M1 marker. In the case of simulation, the curve indicates an increase in the z coordinate, which means that the point in question is moving upwards, while video analysis produces an opposite result (a decrease in the z coordinate. How to explain this discrepancy?

The most plausible answer to that question comes from a close examination of the experiment. During the crash, when the glider is falling down from its acceleration platform, the nose begins to rotate towards the bottom. The rotation is much more intense following a strong bump against the floor and destruction of carriage wheels. It becomes much higher than in the simulation model, where carriage wheels are modeled as rigid (non-destructible) elements. Consequently, the cockpit rotation axis is transferred forward towards the aft in the simulation model. Accordingly, the M1 marker is located on the right side of rotation axis, rather then on its left side (as in the experimental test), and it moves upwards rather then downwards. The conclusion is that the point equivalent to M1 marker was located relatively close to the axis of rotation.

This explanation is further supported by the fact that the simulated movement of the M4 marker, invariably located on the right side of the axis of rotation, is highly consistent with video analysis.

The results of simulation, which reflect the loads applied to the glider's structure and human body, are presented in the following section. Like in the case of experimental test, all signals were filtered in accordance with SAE J211 Standard [18].

3.2. Loads applied to the glider cockpit

Loads applied to the glider's structure were determined by measuring accelerations in two points of the structure: at the rear section of the cockpit and at the frame located under the pilot's seat.

Acceleration recorded in the rear section of the cockpit (Figures 10 and 11), where readings were similar to those stated at the experimental track, while acceleration recorded under the pilot's seat (Figures 12 and 13) was much different from the experimental one.

When comparing the component of acceleration along the direction of movement (Fig. 10), we could observe that a much higher value (47.3 g) was determined from experimental tests than from the simulation (32.7 g). Accordingly, the relative error amounted to 31% in that case. Another important observation is related to the timing. The graph clearly indicates that, compared to the physical model, the simulation model responds with a certain delay to the loads. Timing differences justify the conclusion that the destruction of real structure is much more violent and generates much higher accelerations. The reasons behind different behavior of the simulation model should be sought in inaccurate selection of material parameters of the composite structure, in terms of both fracture-associated and internal damping parameters.

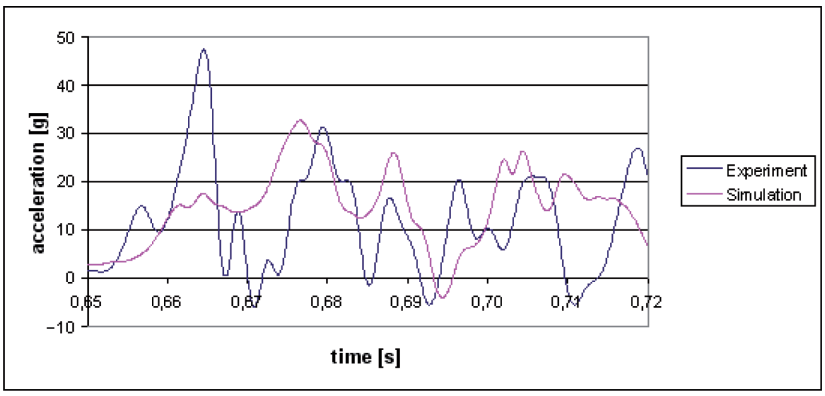

Fig. 10. Acceleration along the direction of motion at the rear section of the pilot's seat

As far as a comparison of vertical components of acceleration in the rear section of the cockpit are concerned (Fig. 11), it can be seen that maximum values yielded by the experiment (33.1 g) and the simulation (42 g) are much less apart than the horizontal components (relative error in the order of 26.8%). It should be noted, however, that the timing is much different and it is impossible to determine time shifts, while maximum acceleration peaks occur in different phases of motion. In addition to the aforementioned errors

in the selection of material parameters, a probable reason should be attributed to a higher rotation of the structure, as observed during the experiment, and certain model imprecision in the rendering (arrangement) of the test track conditions.

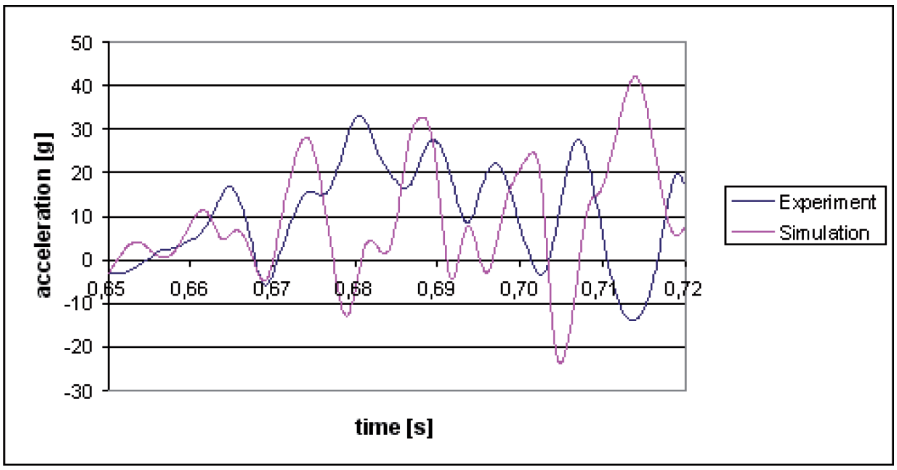

Fig. 11. Vertical acceleration of the rear section of the cockpit

The observation of acceleration development at the frame located beneath the pilot's seat revealed very significant disparities between physical mock-up and simulation model. The differences were reported for both maximum crash acceleration values and the components, both vertical and in the direction of motion. During the experiment, the measured values of the horizontal and vertical components were respectively: 55.1 g and 29.4 g. In the simulation model, these values were several times higher: horizontal and vertical components reached 440 g and 562.1 g, respectively. The curves of acceleration components are compared in Figures 12 and 13.

The question about the reasons behind such a huge difference between experimental and simulation results could be explained by different behavior of the physical mock-up and simulation model, insofar as an anthropometric dummy was used in the simulation model. On the other hand, the dummy used in the experimental test (sewn out of a fabric and filled with sand) fell apart very soon and relieved both pilot's and the frame. Consequently, no fractures or destruction were reported from the seat bucket and frames. In the simulation model, a dummy model Hybrid II used (in practice indestructible) was subjected to a very strong compression (as shown in Figure 4 above) and transferred huge loads to the seat bucket and then to the frames beneath the seat with resulting fractures of the frames. It is reasonable to deem that sudden fracturing of the accelerometer's support is the reason behind the dramatic increase of acceleration.

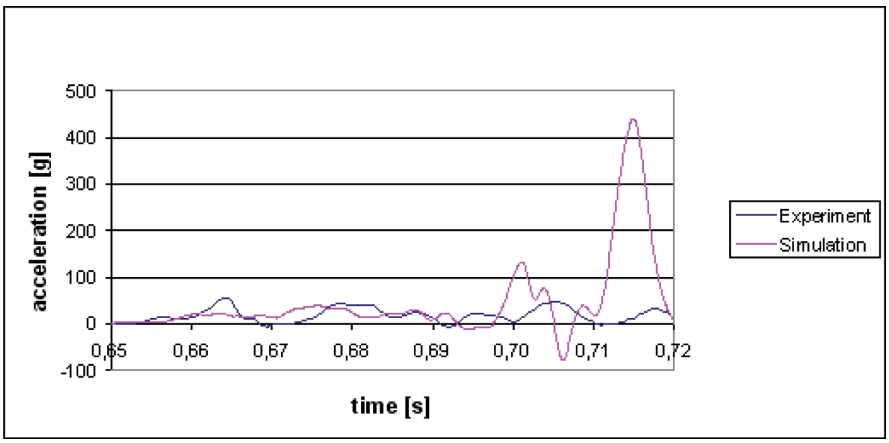

Fig. 12. Acceleration in the direction of motion at the frame beneath the pilot's seat

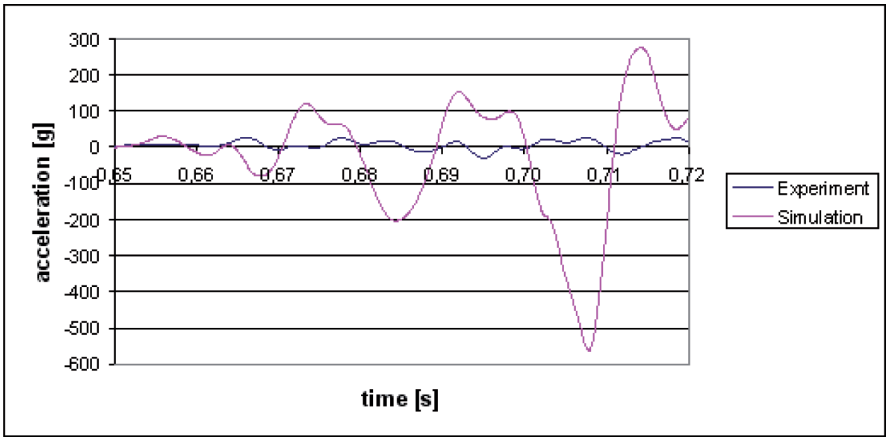

Fig. 13. Vertical acceleration at the frame beneath the pilot's seat

3.3 Loads transferred to the pilot

During the crash, the accelerations of both the head's (Fig. 14) and the chest's (Fig. 15) gravity centers approached respectively 125 g and 180 g. These extremely high values can be explained by the fact that the head hit the body, and the chest was subjected to strong compression by the upper and lower extremities. Accordingly, the loads reached top values in the final phase of the simulation test. The injury criterion calculated for these organs, the so-called *CONTIGUOUS_3MS* (in short CON3ms) amounts to 63.7 g for the head and 138.2 g for the chest, while the limits of tolerance are respectively: 75 g for the head and 60 g for the chest.

The results indicate that head injury criterion CON3ms was not exceeded, in spite of a very high top (peak) acceleration value.

In the case under investigation, the chest injury criterion CON3 ms was more than twice exceeded. This indicates a very high risk of a severe chest injury.

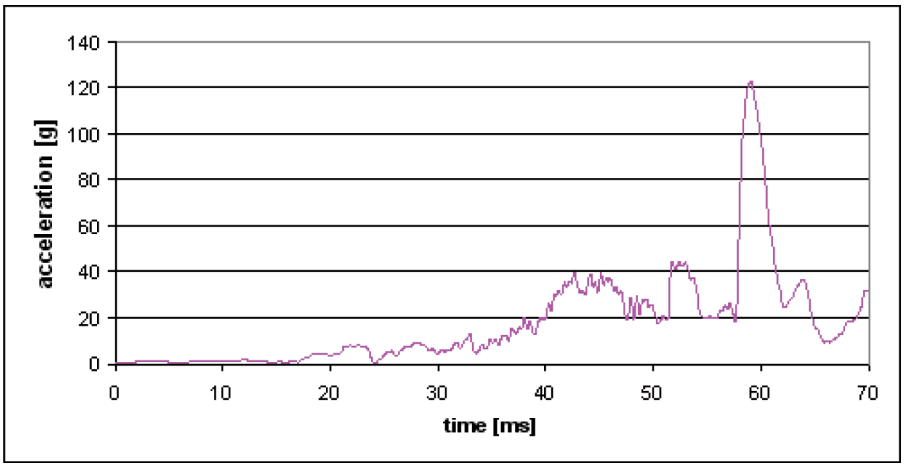

Fig. 14. Acceleration of head's gravity center

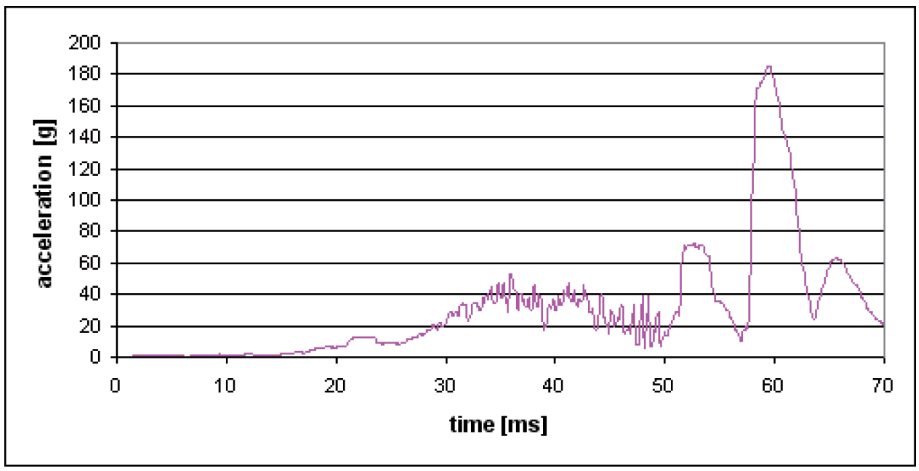

Fig. 15. Chest (sternum) acceleration

Another investigated load to the body, of particular importance in the gliding sport, is the force applied to the lumbar section of the spine (Fig. 16). The permitted load decreases with age, but according to H. Yamada [19] for young pilots, aged 39 or less, it is reasonable to assume a force of 7.14 kN. During the simulation test, however, the force reached a level of almost 64 kN. Therefore, the permitted level was exceeded almost 9-fold. Such a huge force is the result of two factors: first, the body is highly compressed

following the crash and, second – the approach to knapsack modeling as a rigid body sewn into the dummy, bearing additional loads to the spine.

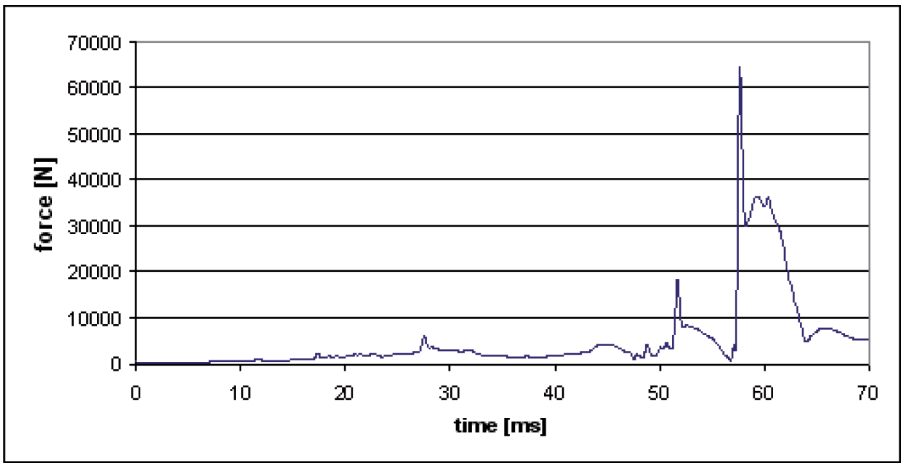

Fig. 16. Axial force at lumbar spine

Another investigated indicator was the compressive force at femur, subsequently used for the assessment of risk to lower extremities (the so-called ***Femur Force Criterion***) [16]. The highest value of that criterion was achieved when legs went into contact with the wall upon destruction of the cockpit's aft section (approx. 24 ms). The results indicated that the loads were transferred in an asymmetric manner, since the force recorded for the left leg was equal to 12.2 kN, while that for the right leg amounted to 14.6 kN. As a general rule, the permitted force level depends on the duration of exposure, but even for a very short time the force may not be higher than 9 kN. Accordingly, the limit was exceeded by approx. 35% for the left leg and by approx. 62% for the right leg.

Finally, the forces at safety belts were investigated as a measure of loads transferred to the pilot (Fig. 17). The standard applicable to four-point safety belts used in aviation [20], according to which these forces should not exceed 8.9 kN, is a certain point of reference to the measured values. The obtained values may seem quite low, but it's probably caused by the fact, that the dummy slipped out of the belts, thus affecting seriously the results. Moreover, it should be mentioned that, because material characteristics for safety belts used in aviation industry were unavailable, the data applicable to automotive safety belts were applied instead.

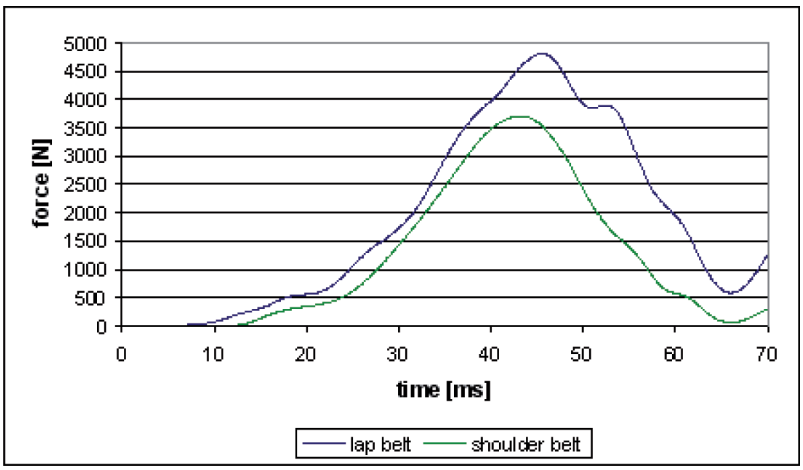

Fig. 17. Forces at safety belts

4. Conclusions

A simulation model of glider crash against a non-deformable barrier at a velocity of v=77 km/h is presented in this paper along with calculated loads transferred to both glider's composite cockpit structure and pilot's body.

In order to ensure experimental verification which allows for quality assessment of the model, a crash test was conducted at a special test track under conditions consistent with the settings of the subsequent simulation [21].

A very simplified model of the glider's composite shell, modeled as an isotropic material subject to destruction upon exceeding critical deformation value (and related energy), was used in the simulation test. Albeit simplified, this approach to modeling seems to be justified in the case of a large structure, such as glider, which is subjected to huge impact loads.

The observation of glider's structure behavior, involving a comparison of test delivery animation with physical experiment, indicates that the numerical model is fairly consistent with the physical experimental model on the level of process kinematics. This is further substantiated by acceleration measurements made in the rear section of the cockpit.

Acceleration measurements under the pilot's seat yielded results that are largely inconsistent with experimental test. This was due to the fact that the simulation dummy was not destructible, unlike physical dummy. The simulation dummy is subjected to severe compression damages through the seat's bucket and the frame to which the accelerometer was attached, thus resulting in an excessive acceleration peak, as measured during the

experimental test. The experimental dummy was completely destroyed, which results in relieving the seat and underlying frames.

Due to the risk of destruction of the anthropometric dummy (Hybrid II), a very simplified dummy was used in the experimental test. Since the dummy made it impossible to measure any loads transferred to the pilot's body, the simulated loads applied to a human body could not be compared with the experimental data – as it was described in this paper,. Therefore, these results should be treated with caution, especially because the range of loads is far beyond the range specified for the anthropometric dummy. Nevertheless, the results may provide a general indication about crash modeling risks.

The simulation revealed that the loads transferred to the human body under this scenario are very high, indeed. Upon almost total destruction of the cockpit, the glider's structure does not provide any protection to the pilot. Immediately upon glider's nose destruction, the pilot's legs come into direct contact with the barrier and the force applied to the tights would, according to the existing criteria, lead to leg fractures. Additional threat arises from strong compression of the entire body, entailing body crushing and consequently significant accelerations of the head and chest. This in combination with loads applied by the legs leads to a high force generated in the lumbar section of the spine. All of these values are high above the permitted human safety limits.

In the light of these results, it is interesting to note that relatively small safety belt forces, much below the limit specified by the standards [20], were reported from the simulation. It seems that this can be attributed to two key reasons. First, it was observed during the simulation that the dummy tended to slip out of the belts. This could decrease significantly the measured forces. Second, the model of belts was based on the characteristics of automotive safety belts, which are more susceptible that those used in gliders.

Selection of material parameters for the investigation of the fracturing process is a weakness of the model. In the model described herein, the parameters were selected on the basis of a single composite sample. In order for the destruction process to be described in a more reliable manner, a series of tests made on simple composite samples should be made and followed by at least simplified optimization [21]. The model will be applied in the future to investigations of crashes against a deformable ground barrier.

Manuscript received by Editorial Board, March 28, 2011;
final version, June 03, 2011.

REFERENCES

[1] European Aviation Safety Agency: CS22. Sailplanes and Powered Sailplanes.
[2] Soaring Safety Foundation: Soaring Safety Foundation Annual Report: 1997-2008, Post Office Box 2100, Hobbs, New Mexico 88241.
[3] Sperber M.: Crashworthiness of glider cockpits, TUV Rheinland, 51105 Koln, Germany.
[4] Bureau of Investigation and Analysis for Civil Aviation Safety: Glider accidents 1999-2001.Study, France, 2001.
[5] Civil Aviation Office: Analiza stanu bezpieczeństwa lotów i skoków spadochronowych w lotnictwie cywilnym RP w 2003 roku, Warsaw, Poland, 2004.
[6] British Gliding Association: Glider accidents in 2008, available at http://www.gliding.co.uk.
[7] Parhi P. K., Bhattacharyya S. K., Sinha P. K.: Failure analysis of multiple delaminated composite plates due to low velocity impact, International Journal of Crashworthiness, Vol. 5, No. 1, 2000, pp. 63-77.
[8] Rao V. V. S., Sinha P. K.: Three dimensional analysis of multidirectional composites subjected to low velocity impact, International Journal of Crashworthiness, Vol. 8, No. 4, 2003, pp. 393-400.
[9] Saito H., Inai R., Hamada H.: Crushing properties of pultruded glass reinforced square tubes, International Journal of Crashworthiness, Vol. 7, No. 1, 2002, pp. 21-32.
[10] Beard S. J., Chang F-K.: Energy absorption of braided composite tubes, International Journal of Crashworthiness, Vol. 7, No. 2, 2002, pp. 191-205.
[11] Mamalis A. G., Manolakos D. E., Ioannidis M. B., Kostazos P. K., Chirwa E. C.: Static and dynamic axial collapse of fibreglass composite thin-walled tubes: finite element modelling of the crush zone, International Journal of Crashworthiness, Vol. 8, No. 3, 2003, pp. 247-254.
[12] Mamalis A. G., Manolakos M. B., Ioannidis M. B., Kostazos P. K.: The bending of fibre-reinforced composite thin-walled tubular components: Numerical modeling, International Journal of Crashworthiness, Vol. 5, No. 2, 2000, pp. 193-205.
[13] Mališ M.: Comparison of hard and soft soil impact surface in glider crashworthiness test simulation, Proc. RRDPAE 2008 – Recent Research and Design Progress in Aeronautical Engineering and its influence on Education, Brno University of Technology, Czech Republic, October 16-17th, 2008.
[14] Manning J. E., Happee R.: Validation of the MADYMO Hybrid II and Hybrid III 50th percentile models in vertical impacts, Presented at Specialists Meeting: Models for aircrew safety assessment: uses, limitations and requirements, Ohio, USA, 26-28 October, 1998.
[15] TASS BV: MADYMO Model Manual. Release 7.1, Delft, The Netherlands, June 2009.
[16] TASS BV: MADYMO Theory Manual. Release 7.1, Delft, The Netherlands, June 2009.
[17] Lindstedt L., Rodzewicz M., Rzymkowski C., Kedzior K.: Experimental Study of Impact Phenomena in the case of a Composite Glider, Technical Soaring, Vol. 33, No. 2/ April–June 2009, pp. 54-62.
[18] SAE International: SAE J 211-1. Revised MAR95.
[19] Yamada H.: Strength of biological materials. Published by F. G. Evans, Williams and Wilkins. Baltimore, Ohio, USA, 1970, pp. 75-80.
[20] European Aviation Safety Agency: CS23. Normal, Utility, Aerobatic and Commuter Aeroplanes.
[21] Lindstedt L.: Dynamical behaviour of a composite cockpit of PW-5 glider when hitting against a ground barrier - the issue of pilot's safety, Ph. D. Thesis, Warsaw University of Technology, Warsaw, 2010.

Symulacja numeryczna zderzenia szybowca z barierą nieodkształcalną

S t r e s z c z e n i e

Niniejsza praca poświęcona została opisowi symulacji komputerowej procesu zderzenia szybowca z nieodkształcalną przeszkodą naziemną, będącej częścią większego projektu, związanego z modelowaniem wypadków szybowcowych. Celem badań było stworzenie numerycznego modelu układu pilot-szybowiec-otoczenie, który uwzględniając dynamikę ciała człowieka oraz kompozytowej struktury kabiny podczas zderzenia, pozwalałby na analizę wypadków lotniczych pod kątem bezpieczeństwa pilota. Jakkolwiek wypadki, w których szybowiec uderza w przeszkodę sztywną (np. ściana) należą do rzadkości, stworzenie modelu symulującego taki przypadek jest bardzo przydatne pod kątem dalszych badań. Po pierwsze, podczas zderzenia ze sztywną barierą proces niszczenia kompozytowej struktury kabiny jest łatwiejszy do zaobserwowania. Ponadto, zastosowanie przeszkody nieodkształcalnej pozwala na wyeliminowanie błędów związanych z modelowaniem odkształcalnego podłoża, co na ogół jest problematyczne. Symulację testu zderzeniowego przeprowadzono w pakiecie MADYMO. Polegał on na zderzeniu szybowca ze ścianą zorientowaną prostopadle do kierunku ruchu przy prędkości 77 km/h. Podczas obliczeń uzyskano przebiegi czasowe sygnałów potrzebnych do oceny zachowania się konstrukcji kabiny pilota oraz ciała człowieka – przyspieszenia i przemieszczenia w wybranych punktach konstrukcji szybowca oraz obciążenia działające na organizm pilota: przyspieszenia głowy i klatki piersiowej, siły w kości udowej, kręgosłupie lędźwiowym i w pasach bezpieczeństwa. Uzyskane wyniki zostały porównane z wynikami przeprowadzonego wcześniej testu eksperymentalnego, służącego weryfikacji modelu numerycznego. W wyniku zderzenia kabina szybowca uległa kompletnemu zniszczeniu, a obciążenia przeniesione na organizm pilota były bardzo duże – przekraczające znacznie dopuszczalne limity. Wykonany model wykazuje dosyć dobrą zgodność z eksperymentem, co pozwala wysnuć wniosek, że w przyszłości może być on wykorzystany do symulacji wypadków lotniczych.